B., Southwick, F. S., Yin, H. L., & Zaner, K. S. (1985) *Annu. Rev. Cell Biol. 1*, 353–402.
Tobacman, L. S., & Korn, E. D. (1983) *J. Biol. Chem. 258*, 3207–3214.
Walsh, T. P., Weber, A., Higgins, J., Bonder, E. M., & Mooseker, M. S. (1984a) *Biochemistry 23*, 2613–2621.
Walsh, T. P., Weber, A., Davis, K., Bonder, E. M., & Mooseker, M. S. (1984b) *Biochemistry 23*, 6099–6102.
Weber, A., Northrop, J., Bishop, M. F., Ferrone, F. A., & Mooseker, M. S. (1987) *Biochemistry* (preceding paper in this issue).
Wegner, A. (1976) *J. Mol. Biol. 108*, 139–150.

Assignment of Fingerprint Vibrations in the Resonance Raman Spectra of Rhodopsin, Isorhodopsin, and Bathorhodopsin: Implications for Chromophore Structure and Environment†

Ilona Palings,‡ Johannes A. Pardoen,§ Ellen van den Berg,§ Chris Winkel,§ Johan Lugtenburg,§ and Richard A. Mathies*,‡

Chemistry Department, University of California, Berkeley, California 94720, and Chemistry Department, Gorlaeus Laboratories, Leiden University, 2300 RA Leiden, The Netherlands

Received August 22, 1986; Revised Manuscript Received December 12, 1986

ABSTRACT: ^{13}C- and ^{2}H-labeled retinal derivatives have been used to assign normal modes in the 1100–1300-cm^{-1} fingerprint region of the resonance Raman spectra of rhodopsin, isorhodopsin, and bathorhodopsin. On the basis of the ^{13}C shifts, C_8–C_9 stretching character is assigned at 1217 cm^{-1} in rhodopsin, at 1206 cm^{-1} in isorhodopsin, and at 1214 cm^{-1} in bathorhodopsin. C_{10}–C_{11} stretching character is localized at 1098 cm^{-1} in rhodopsin, at 1154 cm^{-1} in isorhodopsin, and at 1166 cm^{-1} in bathorhodopsin. C_{14}–C_{15} stretching character is found at 1190 cm^{-1} in rhodopsin, at 1206 cm^{-1} in isorhodopsin, and at 1210 cm^{-1} in bathorhodopsin. C_{12}–C_{13} stretching character is much more delocalized, but the characteristic coupling with the $C_{14}H$ rock allows us to assign the "C_{12}–C_{13} stretch" at ~1240 cm^{-1} in rhodopsin, isorhodopsin, and bathorhodopsin. The insensitivity of the C_{14}–C_{15} stretching mode to N-deuteriation in all three pigments demonstrates that each contains a trans (anti) protonated Schiff base bond. The relatively high frequency of the C_{10}–C_{11} mode of bathorhodopsin demonstrates that bathorhodopsin is s-trans about the C_{10}–C_{11} single bond. This provides strong evidence against the model of bathorhodopsin proposed by Liu and Asato [Liu, R., & Asato, A. (1985) *Proc. Natl. Acad. Sci. U.S.A. 82*, 259], which suggests a C_{10}–C_{11} s-cis structure. Comparison of the fingerprint modes of rhodopsin (1098, 1190, 1217, and 1239 cm^{-1}) with those of the 11-*cis*-retinal protonated Schiff base in methanol (1093, 1190, 1217, and 1237 cm^{-1}) shows that the frequencies of the C–C stretching modes are largely unperturbed by protein binding. In particular, the invariance of the C_{14}–C_{15} stretching mode at 1190 cm^{-1} does not support the presence of a negative protein charge near C_{13} in rhodopsin. In contrast, the frequencies of the C_8–C_9 and C_{14}–C_{15} stretches of bathorhodopsin and the C_{10}–C_{11} and C_{14}–C_{15} stretches of isorhodopsin are significantly altered by protein binding. The implications of these observations for the mechanism of wavelength regulation in visual pigments and energy storage in bathorhodopsin are discussed.

Rhodopsin, the major protein in the disc membranes of retinal rod cells, is the pigment responsible for black and white vision in vertebrates. The amino acid sequence of bovine rhodopsin has been determined (Hargrave et al., 1983; Ovchinnikov, 1982), and the secondary structure is thought to consist of seven transmembrane α-helices (Chabre, 1985). Rhodopsin contains an 11-*cis*-retinal chromophore bound to lysine-296 via a protonated Schiff base bond. Upon absorption of light the chromophore photoconverts to the all-trans isomer (I) forming the primary photoproduct bathorhodopsin, which

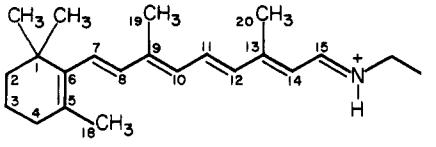

I

decays thermally via a series of metastable intermediates (Yoshizawa & Wald, 1963). The metarhodopsin II form catalyzes the activation of the enzyme transducin (Bennett et al., 1982), which carries the excitation signal to a phosphodiesterase (Stryer, 1986). The consequent reduction in the cytoplasmic cGMP level effects a closure of the sodium channels of the plasma membrane and results in the hyper-

† Work in Berkeley was supported by a grant from the National Institutes of Health (EY-02051). Work in Leiden was supported by grants from The Netherlands Organization for the Advancement of Pure Research (ZWO) and The Netherlands Foundation for Chemical Research (SON). R.A.M. is an NIH Research Career Development Awardee (EY-00219). Preliminary accounts of this work were presented at the 29th and 30th Annual Meetings of the Biophysical Society, February 1985 and 1986.

* Author to whom correspondence should be addressed.
‡ University of California.
§ Leiden University.

0006-2960/87/0426-2544$01.50/0

polarization of the rod cell (Haynes et al., 1986; Zimmerman & Baylor, 1986).

To understand the molecular mechanism of the primary photoprocess, it is necessary to determine the structure of the retinal chromophore in rhodopsin and bathorhodopsin and to identify important chromophore–protein interactions. Two properties of these pigments are of particular interest. The first is the "opsin shift" of the absorption maximum of the 11-*cis*-retinal protonated Schiff base (PSB)[1] chromophore from ~440 nm in methanol to 498 nm in the protein. Experiments with dihydroretinal-containing pigments and theoretical calculations suggest that this red shift results from the interaction of a negatively charged protein residue with the chromophore near the C_{13} position (Arnaboldi et al., 1979; Honig et al., 1979a). Second, bathorhodopsin has an enthalpy content 36 kcal/mol higher than rhodopsin (Cooper, 1979; Boucher & LeBlanc, 1985). This is nearly 60% of the energy of the absorbed photon. Theoretical studies have investigated the possibility of electrostatic energy storage via the protonated Schiff base and of energy storage via conformational distortion of the chromophore (Honig et al., 1979b; Warshel & Barboy, 1982; Birge & Hubbard, 1980, 1981). Experimentally, several clues to the mechanism of energy storage have been uncovered. The resonance Raman spectrum of bathorhodopsin shows unusually intense hydrogen out-of-plane wagging vibrations in the 800-920-cm^{-1} region, which indicate that the chromophore is conformationally distorted (Eyring et al., 1980; Warshel & Barboy, 1982). These modes have been assigned to the $C_{10}H$, $C_{11}H$, $C_{12}H$, and $C_{14}H$ wagging vibrations. Furthermore, the unusual uncoupling of the $C_{11}H$ and $C_{12}H$ wags in bathorhodopsin suggests that the chromophore is strongly perturbed by the protein near C_{12} (Eyring et al., 1982).

In this paper we investigate three aspects of chromophore structure that are important for the mechanisms of wavelength regulation and energy storage. First, we want to determine the configuration and environment of the C=NH moiety in rhodopsin, isorhodopsin, and bathorhodopsin. Models for electrostatic energy storage have made the assumption that the electrostatic environment of the Schiff base in bathorhodopsin is significantly different from that in rhodopsin. This assumption depends on the position and orientation of the protonated Schiff base inside the binding pocket, which is determined in part by the C=N configuration. Second, the conformation of chromophore C–C single bonds has recently become an important issue. A model has been proposed for the rhodopsin → bathorhodopsin conversion in which bathorhodopsin contains a C_{10}–C_{11} s-cis bond (Liu & Asato, 1985). Such a structure would profoundly alter our picture of visual photochemistry if proven to be correct. Third, it is important to define the nature and location of protein–chromophore interactions. Charged residues near the chromophore and conformational distortions can be involved in the opsin shift and energy storage mechanisms.

These aspects of chromophore structure can be investigated with resonance Raman spectroscopy of isotopically labeled visual pigments. Assigning the normal modes of the chromophore allows us to uncover characteristic frequencies and coupling patterns that are sensitive to structure. In making these assignments we have drawn on the recent vibrational analysis of the various retinal isomers (Curry et al., 1982, 1985), the *all-trans*-retinal PSB (Smith et al., 1985), BR_{548} (Smith et al., 1987c), and BR_{568} (Smith et al., 1987b). These studies have led to the development of vibrational methods for determining the configuration of the C=C and C=N bonds and the conformation of C–C single bonds in retinal-containing pigments (Smith et al., 1984, 1986).

In this work, ^{13}C- and ^{2}H-labeled retinal chromophores were used to assign normal modes in the fingerprint region of the Raman spectra of rhodopsin, bathorhodopsin, isorhodopsin, and their PSB model compounds. Resonance Raman spectra of rhodopsin were obtained at room temperature with a rapid-flow method. Spectra of bathorhodopsin and isorhodopsin were obtained at 77K with a spinning cell technique (Braiman & Mathies, 1982). The vibrational assignments allow us to conclude that the C=N configuration is trans (anti) in rhodopsin and is unchanged in bathorhodopsin and isorhodopsin in agreement with preliminary findings from our laboratory (Palings et al., 1985) and Fourier-transform infrared (FTIR) results (Bagley et al., 1985). Comparison of the frequencies and isotopic shifts of the C_{10}–C_{11} mode of bathorhodopsin and of the all-trans PSB shows that bathorhodopsin has a C_{10}–C_{11} s-trans single bond, in support of FTIR (Bagley et al., 1985) and recent chemical analogue studies (Asato et al., 1986; Sheves et al., 1986). Finally, we do not observe evidence for localized perturbations in the fingerprint region of rhodopsin. However, perturbations of the C–C stretching modes *are* observed in the spectra of bathorhodopsin and isorhodopsin.

Materials and Methods

Model Compound Preparation. The synthesis and characterization of the 9-^{13}C, 10,11-^{13}C, 13-^{13}C, 15-^{13}C, 14,15-^{13}C, $C_{10}D$, $C_{14}D$, and $C_{20}D_3$ derivatives of retinal have been described by Lugtenburg and co-workers [Pardoen et al., 1986; Lugtenburg (1985) and references cited therein]. The $C_{14}D$ all-trans PSB was synthesized and the Raman spectrum of the microcrystalline precipitate of the chloride salt obtained as previously described (Smith et al., 1985). The 9-*cis*-retinal Schiff bases were synthesized by reaction of ~1 mg of retinal with a 20-fold excess of *n*-butylamine in 1 mL of hexane at room temperature for 15 min. Subsequently, the solvent and the excess *n*-butylamine were evaporated under a stream of nitrogen, and the residue was dissolved in ~10 mL of CCl_4. The solution was titrated with ~200 μL of an acidified (12 M HCl) solution of methanol until a stable 9-cis PSB had formed as assayed by absorption spectroscopy. In CCl_4 solution the 9-cis PSB has significantly narrower vibrational line widths than in methanol. The 11-*cis*-retinal protonated Schiff bases were unstable in CCl_4 and were therefore prepared in methanol. After 15 min the reaction mixture was diluted with ~8 mL of methanol and titrated with acidified methanol until a stable PSB had formed. The presence of excess *n*-butylamine was found to be essential for the stability of the 11-cis PSB. 9-Cis- and all-trans PSB fingerprint frequencies for the correlation diagrams were obtained from spectra recorded in methanol following the same procedure employed for the 11-cis PSB.

Pigment Preparation. One hundred thawed bovine retinas (J. A. Lawson, Lincoln, NE) were suspended in 100 mL (40% w/w) of sucrose in MOPS buffer (20 mM MOPS, 1 mM $CaCl_2$, 0.2 mM EDTA, pH 7.4) and vortexed for 30 s. The suspension was then centrifuged at 6000 rpm (4000*g*) in a Beckman J-21 centrifuge for 20 min to pellet most of the debris. The supernatant was diluted in half with MOPS buffer, and the rod outer segments were pelleted for 30 min at 12000 rpm (17000*g*). The pellets were collected and vortexed to give a thick suspension (~25 mL), which was

[1] Abbreviations: RR, resonance Raman; SB, Schiff base; PSB, protonated Schiff base; HOOP, hydrogen out of plane; MOPS, 3-(*N*-morpholino)propanesulfonic acid; EDTA, ethylenediaminetetraacetic acid.

loaded onto three sucrose gradients [50 mL, 20–40% (w/w) sucrose in MOPS buffer]. Density gradient centrifugation in a Beckman L8-70 ultracentrifuge at 25 000 rpm (107000*g*) for 2 h results in the resolution of two bands in the gradient. The upper one containing the rod outer segments was collected, diluted in half with MOPS buffer, and centrifuged at 12 000 rpm (17000*g*) for 30 min. The yield was typically 10–15 nmol of rhodopsin/retina (ϵ_{max} 40 000 cm^{-1} M^{-1}). The isolated rod outer segments were lysed in water and bleached in 100 mM phosphate buffer containing 10 mM NH_2OH. The bleached rod outer segments were washed twice with phosphate buffer to remove excess hydroxylamine. Pigments were regenerated in 100 mM phosphate buffer for 90 min at room temperature with labeled 9-*cis*- or 11-*cis*-retinals. The regenerated pigments were dissolved in an Ammonyx-LO detergent solution (Onyx Chemical Co., Jersey City, NJ) and purified by hydroxylapatite chromatography (Applebury et al., 1974). For low-temperature spectroscopy (77K) the purified pigment was concentrated with Amicon CF25 centriflo membrane cones (Danvers, MA) to approximately 0.5 mL (40 OD/cm at 500 nm). Deuteriated samples were obtained by washing the concentrated pigment solution twice with D_2O in the Amicon centriflo cones.

Resonance Raman Flow Experiments. Room temperature rapid-flow resonance Raman (RR) spectra of rhodopsin and isorhodopsin were obtained with 10–15 mL of sample having an absorbance of 1.0–1.5 OD/cm at 500 nm (100 mM phosphate buffer, 10 mM NH_2OH, <1% Ammonyx-LO). Raman scattering was excited with the 488-nm line of a Spectra-Physics 2020 argon ion laser. The laser power (400 μW), flow rate (400 cm/s), and beam diameter (10 μm) were chosen to make the effects of photolysis on the spectra negligible (photoalteration parameter $F \sim 0.1$; Mathies et al., 1976).

Room temperature RR spectra of 9-cis PSB and 11-cis PSB were obtained with 488-nm (3-mW) and 514.5-nm (1.5-mW) excitation, respectively. Spectra of 9-cis PSB were collected in two 1-min integrations in a single-pass flow experiment (flow rate ~225 cm/s; beam diameter 10 μm; ϵ_{max} 39 400; $\phi \leq 0.05$; $F \leq 0.06$). Spectra of 11-cis PSB were collected in two 1-min integrations with a recirculating flow system (flow rate 700 cm/s; beam waist 10 μm; ϵ_{max} 23 300 M^{-1} cm^{-1}; $\phi = 0.25$; $F = 0.02$). The extinction coefficient (ϵ) and quantum yield (ϕ) values are from Freedman and Becker (1986). The Raman scattering was detected with a dry ice cooled intensified vidicon detector (PAR 1205A/1205D) coupled to a subtractive dispersion double spectrometer. The spectrometer was calibrated with cyclohexene as an external standard. The spectral slit width was 6–8 cm^{-1}. Frequencies are accurate to ±3 cm^{-1}.

Low-Temperature RR Experiments. To obtain RR spectra of bathorhodopsin, we used a 77K spinning sample technique (Braiman & Mathies, 1982). Approximately 50 μL of concentrated pigment solution was frozen in a groove of the cold conical copper tip and spun at 1500 rpm. The sample was irradiated with a 476-nm pump beam (200 mW) from a Spectra-Physics 2020 argon ion laser, creating a photostationary steady-state mixture containing approximately 22% rhodopsin, 65% bathorhodopsin, and 13% isorhodopsin (Suzuki & Callender, 1981). The relative concentrations are dictated by the extinction coefficients and photochemical quantum yields according to the following kinetic scheme:

$$\text{11-}cis\text{-rhodopsin} \underset{h\nu}{\overset{h\nu}{\rightleftharpoons}} \textit{all-trans}\text{-bathorhodopsin} \underset{h\nu}{\overset{h\nu}{\rightleftharpoons}} \text{9-}cis\text{-isorhodopsin}$$

Subsequently, the sample was rotated to a low-photoalteration 568-nm probe beam (5–10 mW, 50-mm lens) from a Spectra-Physics 171 krypton ion laser, which selectively enhanced the Raman scattering from bathorhodopsin. The essential advantage of this method over previously published methods (Oseroff & Callender, 1974) is the large increase in the signal to noise ratio due to elimination of fluorescence excited by the pump beam and elimination of line-broadening effects presumably due to heating of the sample. This allows us to reduce the probe laser power to a low level so that scattering from rhodopsin and isorhodopsin is minimized. Consequently, high-quality spectra of bathorhodopsin are obtained. RR spectra of isorhodopsin at 77K were obtained by probing the spinning sample with a 568-nm laser beam (50–70 mW), which both produces isorhodopsin and excites the Raman scattering. The Raman scattering was detected with a standard photon-counting Raman system. The double monochromator was calibrated on the 568-nm Rayleigh line, and spectral slit widths were 2 cm^{-1}. Frequencies are accurate to ±2 cm^{-1}. The spectra were corrected for spectrometer sensitivity, and fluorescence backgrounds were subtracted with a quartic background fitting algorithm.

Table I: *all-trans*-Retinal Protonated Schiff Base Vibrational Frequencies[a]

derivative	fingerprint frequency (cm^{-1})			
unmodified	1159	1191	1204	1237
9-^{13}C	1156 (−3)	*b*	1195 (−9)	1236 (−1)
10,11-^{13}C	1147 (−12)	1185 (−6)	1202 (−2)	1235 (−2)
13-^{13}C	1156 (−3)	1189 (−2)	1203 (−1)	1230 (−7)
14,15-^{13}C	*b*	1172 (−19)	1204 (0)	1234 (−3)
$C_{10}D$[c]	1156 (−3)	1189 (−2)	1279 (+75)	1230 (−7)
$C_{14}D$	1152 (−7)	1184 (−7)	1210 (+6)	1304 (+67)

[a] Shifts from unmodified *all-trans*-retinal PSB are given in parentheses. Spectra were obtained from a microcrystalline precipitate. ^{13}C data are reproduced from Smith et al. (1985). [b] Not resolved. [c] From Smith (1985).

RESULTS

First, we will discuss the vibrational assignments for the *all-trans*, 11-*cis*, and 9-*cis*-retinal PSB model compounds and compare these assignments with those for bathorhodopsin, rhodopsin, and isorhodopsin. Subsequently, data addressing the configuration and environment of the protonated Schiff base bond in the pigments are presented.

all-trans-Retinal PSB. The normal modes of the *all-trans*-retinal PSB have been assigned previously, and a detailed normal coordinate analysis has been presented (Smith et al., 1985). To facilitate comparison with bathorhodopsin, a selected set of isotopic derivative spectra is reproduced in Figure 1. The isotopic shifts of the modes are presented in Table I. In the 1100–1250-cm^{-1} fingerprint region, the C_{10}–C_{11} and C_{14}–C_{15} stretching coordinates are relatively localized in particular normal modes. They can be unambiguously assigned with 10,11-^{13}C and 14,15-^{13}C substitution.[2] The C_{10}–C_{11} stretch is assigned at 1159 cm^{-1} on the basis of the 12-cm^{-1} shift of this mode in the 10,11-^{13}C derivative. The C_{14}–C_{15} stretch is assigned at 1191 cm^{-1} on the basis of its 19 cm^{-1} shift in the 14,15-^{13}C derivative. Substitutions at positions 9 and 13 cause shifts in normal modes containing the C_8–C_9

[2] C_{10}–C_{11} and C_{14}–C_{15} stretching character will also be associated with normal modes involving the bonded C=C stretches and C–C–H rocks so that the distribution of C–C stretch character among all the normal modes of the molecule is complicated. However, if we focus on the distribution of C_{10}–C_{11} or C_{14}–C_{15} stretch character over just the 1100–1250-cm^{-1} skeletal modes, the ^{13}C isotopic shifts clearly show that these internal coordinates are "localized" in particular normal modes.

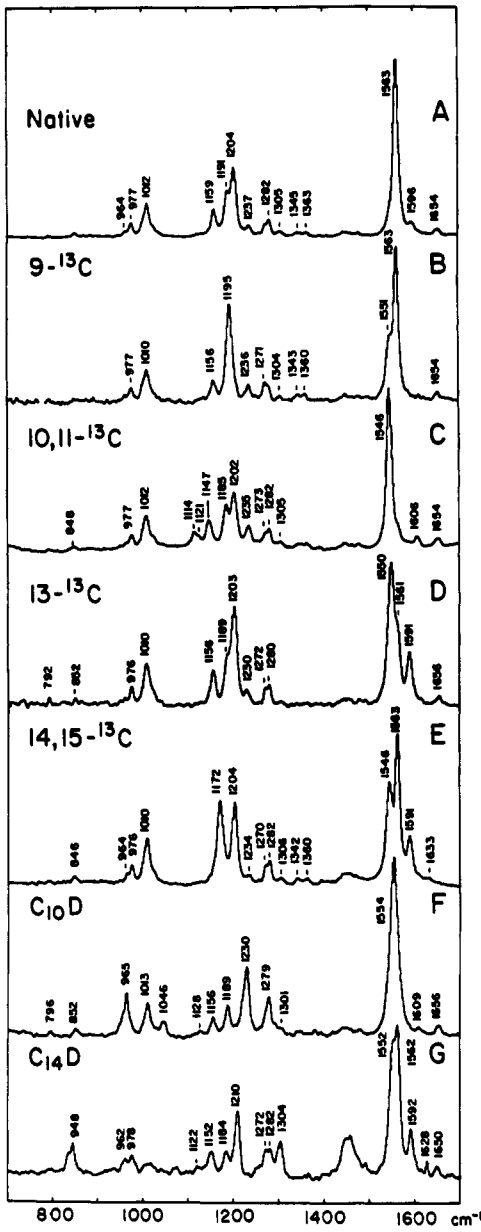

FIGURE 1: Raman spectra of (A) *all-trans*-retinal protonated Schiff base and its (B) 9-^{13}C, (C) 10,11-^{13}C, (D) 13-^{13}C, (E) 14,15-^{13}C, (F) $C_{10}D$, and (G) $C_{14}D$ derivatives. Spectra A–E are from Smith et al. (1985). Spectrum F is from Smith (1985). Spectra were obtained from microcrystalline precipitates of the chloride salt at room temperature with 752-nm excitation.

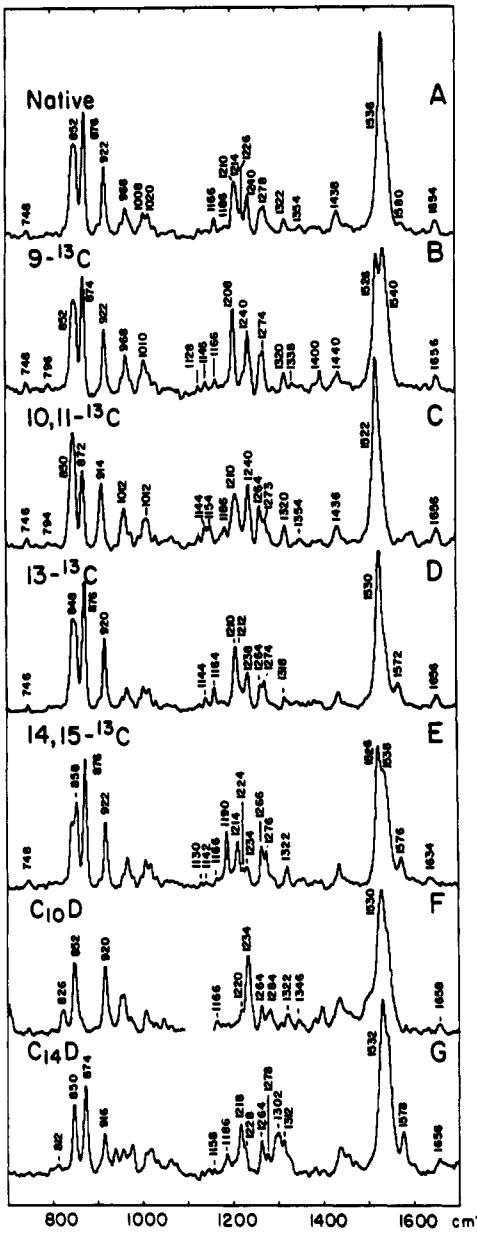

FIGURE 2: Raman spectra of (A) bathorhodopsin and its (B) 9-^{13}C, (C) 10,11-^{13}C, (D) 13-^{13}C, (E) 14,15-^{13}C, (F) $C_{10}D$, and (G) $C_{14}D$ derivatives (568-nm probe). The $C_{10}D$ spectrum is reproduced from Eyring et al. (1982).

and C_{12}–C_{13} stretching coordinates. The C_8–C_9 stretch is assigned at 1204 cm^{-1} on the basis of its 9-cm^{-1} shift in the 9-^{13}C derivative. Similarly, the 7-cm^{-1} shift of the 1237-cm^{-1} band in the 13-^{13}C derivative allows us to assign the C_{12}–C_{13} stretch at 1237 cm^{-1}.

Assignment of a normal mode as a localized C_8–C_9 (or C_{12}–C_{13}) stretch by means of ^{13}C substitution is not always possible. Sometimes the ^{13}C-induced shifts are small and are delocalized over several normal modes, indicating that C_8–C_9 (or C_{12}–C_{13}) stretch character is delocalized. In this case, we will use the strong *characteristic* coupling of the $C_{10}H$ (or $C_{14}H$) rock with the C_8–C_9 (or C_{12}–C_{13}) stretching coordinate to assign the "C_8–C_9 mode" (or "C_{12}–C_{13} mode"). A large (~80-cm^{-1}) upshift of the C_8–C_9 (or C_{12}–C_{13}) mode is expected when $C_{10}H$ (or $C_{14}H$) is deuteriated (Curry et al., 1982, 1985). In $C_{10}D$ all-trans PSB, a 75-cm^{-1} shift of the 1204-cm^{-1} C_8–C_9 mode to 1279 cm^{-1} is observed, and in $C_{14}D$ all-trans PSB there is a 67-cm^{-1} shift of the 1237-cm^{-1} C_{12}–C_{13} mode to 1304 cm^{-1}. This effect provides a consistency check on the assignments of these normal modes in the all-trans PSB, and it will be used in assigning the more complicated spectra discussed below.

Table II: Bathorhodopsin Vibrational Frequencies[a]

derivative	fingerprint frequency (cm^{-1})			
unmodified	1166	1210[b]	1214[b]	1240[b]
9-^{13}C	1166 (0)	1208 (-2)	1208 (-6)	1240 (0)
10,11-^{13}C	1154 (-12)	1210[b] (0)	1214[b] (0)	1240[b] (0)
13-^{13}C	1164 (-2)	1210[b] (0)	1212[b] (-2)	1238[b] (-2)
14,15-^{13}C	1166 (0)	1190 (-20)	1214 (0)	1234 (-6)
$C_{10}D$	1166 (0)	1220 (+10)	1284 (+70)	1234 (-6)
$C_{14}D$	1158 (-8)	1186 (-24)	1218 (+4)	1302 (+62)

[a] Shifts from unmodified bathorhodopsin are given in parentheses. [b] Frequency was determined by Lorentzian deconvolution.

Bathorhodopsin. The normal modes to be assigned are those at 1166, 1210, 1214 (sh), and 1240 cm^{-1} (Figure 2 and Table II). The existence of two modes at 1210 and 1214 cm^{-1} is demonstrated by Lorentzian band deconvolution and by iso-

Table III: 11-*cis*-Retinal Protonated Schiff Base Vibrational Frequencies[a]

derivative	fingerprint frequency (cm^{-1})				
unmodified	1093	1190	1217	1237	1276
9-^{13}C	1093 (0)	1187[b] (−3)	1203[b] (−14)	1235 (−2)	1275 (−1)
10,11-^{13}C	*c*	1185 (−5)	1216 (−1)	1237 (0)	1272 (−4)
13-^{13}C	1094 (+1)	1192[b] (+2)	1210[b] (−7)	1234[b] (−3)	1274 (−2)
14,15-^{13}C	1093 (0)	1173 (−17)	1216[b] (−1)	1233[b] (−4)	1275 (−1)
$C_{10}D$	1092 (−1)	1189 (−1)	1295 (+78)	1232 (−5)	1273 (−3)
$C_{14}D$	1099 (+6)	1182 (−8)	1221[b] (+4)	1319 (+82)	1272 (−4)

[a] Shifts from unmodified 11-*cis*-retinal PSB are given in parentheses. Spectra were obtained in methanol solution. [b] Frequency was determined by Lorentzian deconvolution. [c] Not observed.

topic derivative data (see below). In 10,11-^{13}C bathorhodopsin, a 12-cm^{-1} shift of the 1166-cm^{-1} line down to 1154 cm^{-1} is observed. This shift is identical with that observed in the all-trans PSB (1159 → 1147 cm^{-1}), and the C_{10}–C_{11} stretch can therefore be assigned with confidence at 1166 cm^{-1}. As in the PSB, the downshifted C_{10}–C_{11} stretch mixes with and donates intensity to ionone ring modes at 1128 and 1144 cm^{-1} (Smith et al., 1985). C_{14}–C_{15} stretching character resides predominantly at 1210 cm^{-1}, since this line shifts down 20 cm^{-1} to 1190 cm^{-1} in 14,15-^{13}C bathorhodopsin. This shift is also virtually identical with that observed for the all-trans PSB. Some C_{14}–C_{15} stretching character is also found in the 1240-cm^{-1} mode, since this line shifts down by 6 cm^{-1}. The downshift of the C_{14}–C_{15} stretch clearly reveals the 1214-cm^{-1} line. This line can be characterized as the C_8–C_9 stretch on the basis of its ~6-cm^{-1} downshift to 1208 cm^{-1} in 9-^{13}C bathorhodopsin into coincidence with the C_{14}–C_{15} stretch. The $C_{10}D$ bathorhodopsin spectrum provides additional evidence for C_8–C_9 stretch contribution to the 1214-cm^{-1} mode. Deuteriation causes a loss of intensity at ~1214 cm^{-1} and an increase of intensity at ~1284 cm^{-1}. The band at 1220 cm^{-1} in the $C_{10}D$ derivative is presumably the C_{14}–C_{15} stretch. C_{12}–C_{13} stretching character is delocalized over the modes at 1240, 1214, and 1166 cm^{-1} as demonstrated by their 2-cm^{-1} shifts in 13-^{13}C bathorhodopsin. However, only the 1240-cm^{-1} line exhibits the characteristic coupling with the $C_{14}H$ rock. Intensity shifts from 1240 to ~1302 cm^{-1} in the $C_{14}D$ derivative, similar to the behavior of this mode in $C_{14}D$ all-trans PSB. Hence, we characterize the 1240-cm^{-1} mode as the "C_{12}–C_{13} stretch".

11-cis-Retinal PSB. The Raman spectra of the 11-cis PSB derivatives are given in Figure 3, and the isotopic shifts are summarized in Table III. C_{14}–C_{15} stretching character is localized in the 1190-cm^{-1} mode as indicated by the 17-cm^{-1} shift of this line in the 14,15-^{13}C derivative. We assign the 1093-cm^{-1} mode to the C_{10}–C_{11} stretch on the basis of its correspondence with the 1084-cm^{-1} C_{10}–C_{11} stretch in 11-cis-retinal (Curry et al., 1985) and its disappearance in the 10,11-^{13}C derivative. C_8–C_9 stretching character is predominantly localized in the mode at 1217 cm^{-1} as evidenced by its 14-cm^{-1} downshift in the 9-^{13}C derivative. The shift of intensity from 1217 to 1295 cm^{-1} in the $C_{10}D$ spectrum supports this assignment. The shifts in the 13-^{13}C spectrum indicate that C_{12}–C_{13} stretching character is delocalized over several fingerprint modes (Table III). Although the largest shift is observed in the 1217-cm^{-1} mode, only the mode at 1237 cm^{-1} shows the characteristic coupling with the $C_{14}H$ rock, shifting up to ~1319 cm^{-1} in the $C_{14}D$ derivative. Hence, we label the 1237-cm^{-1} mode the "C_{12}-C_{13} stretch".

Rhodopsin. RR spectra of rhodopsin and its derivatives are presented in Figure 4, and the isotopic shifts are summarized in Table IV. The C_{14}–C_{15} stretch is assigned at 1190 cm^{-1}, on the basis of the 22-cm^{-1} shift of this line in 14,15-^{13}C rhodopsin. The C_{14}–C_{15} stretching coordinate also contributes

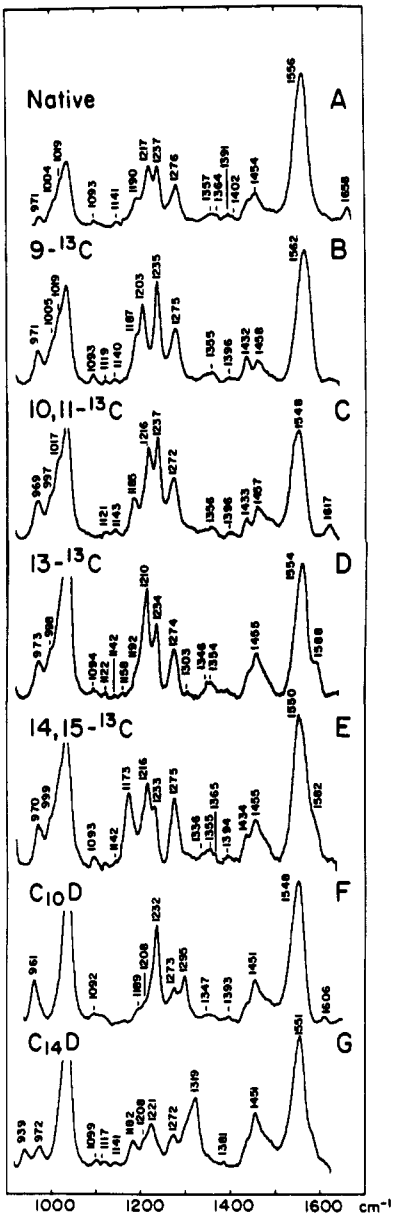

FIGURE 3: Raman spectra of (A) 11-*cis*-retinal protonated Schiff base in methanol solution and its (B) 9-^{13}C, (C) 10,11-^{13}C, (D) 13-^{13}C, (E) 14,15-^{13}C, (F) $C_{10}D$, and (G) $C_{14}D$ derivatives.

significantly to the normal mode at 1239 cm^{-1}. In 10,11-^{13}C rhodopsin, intensity disappears at 1098 cm^{-1}, and a new weak line appears at 1079 cm^{-1}, which is presumably the shifted 1098-cm^{-1} mode. The frequency and ^{13}C shift of this mode are similar to those of the C_{10}–C_{11} mode in 11-*cis*-retinal, which shifts from 1084 to 1063 cm^{-1} in the 10,11-^{13}C derivative (Curry et al., 1985). We therefore assign the C_{10}–C_{11} stretch in rhodopsin at 1098 cm^{-1}. The C_8–C_9 stretch is assigned at 1217 cm^{-1} on the basis of the 14-cm^{-1} shift of this band in 9-^{13}C

Table IV: Rhodopsin Vibrational Frequencies[a]

derivative	fingerprint frequency (cm^{-1})				
unmodified	1098	1190	1217	1239	1270
9-^{13}C	1094 (−4)	1189 (−1)	1203 (−14)	1237 (−2)	1266 (−4)
10,11-^{13}C	1079 (−19)	1184 (−6)	1213 (−4)	1237 (−2)	1265 (−5)
13-^{13}C	1095 (−3)	1191 (+1)	1211 (−6)	1234 (−5)	1264 (−6)
14,15-^{13}C	1093 (−5)	1168 (−22)	1213[b] (−4)	1227[b] (−12)	1265 (−5)
$C_{10}D$	1098 (0)	*c*	1306 (+89)	1236 (−3)	1264 (−6)
$C_{14}D$	1099 (+1)	1186 (−4)	1216 (−1)	1310 (+71)	1264 (−6)

[a] Shifts from unmodified rhodopsin are given in parentheses. [b] Frequency was determined by Lorentzian deconvolution. [c] Not observed.

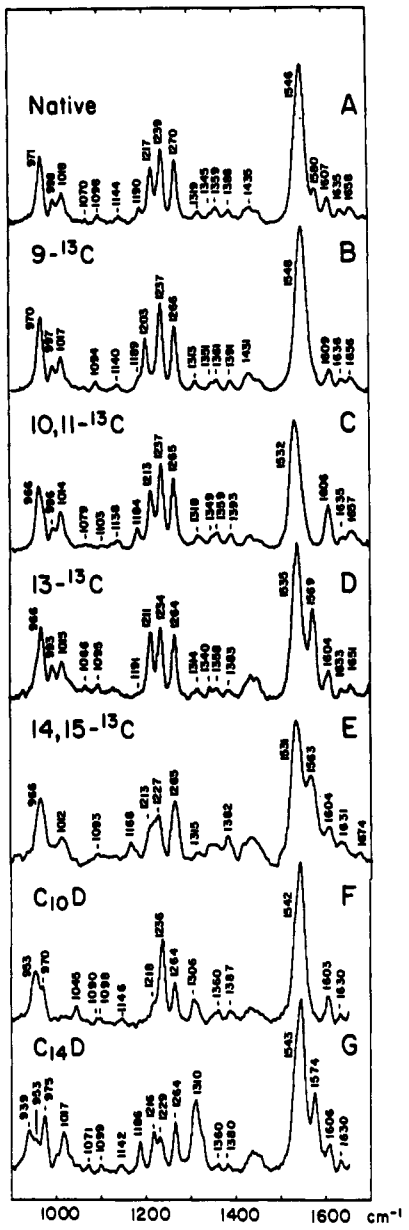

FIGURE 4: Room temperature rapid-flow Raman spectra of (A) rhodopsin and its (B) 9-^{13}C, (C) 10,11-^{13}C, (D) 13-^{13}C, (E) 14,15-^{13}C, (F) $C_{10}D$, and (G) $C_{14}D$ derivatives (488-nm probe).

rhodopsin. This assignment is consistent with the observed loss of intensity at 1217 cm^{-1} and increase of intensity at 1306 cm^{-1} in the $C_{10}D$ pigment. The isotopic shifts observed in the 13-^{13}C spectrum indicate that the C_{12}–C_{13} stretching coordinate in rhodopsin contributes to four normal modes in the C–C stretch region. However, only the mode at 1239 cm^{-1} exhibits the characteristic coupling with the $C_{14}H$ rocking coordinate, shifting up by 71 cm^{-1} in $C_{14}D$ rhodopsin. Hence, we assign the "C_{12}–C_{13} stretch" at 1239 cm^{-1}.[3]

Table V: 9-*cis*-Retinal Protonated Schiff Base Vibrational Frequencies[a]

derivative	fingerprint frequency (cm^{-1})			
unmodified	1134	1189[b]	1203[b]	1237
9-^{13}C	1130 (−4)	1188[b] (−1)	1198[b] (−5)	1236 (−1)
10,11-^{13}C	1114 (−20)	1184 (−5)	1200 (−3)	1234 (−3)
13-^{13}C	1136 (+2)	1188[b] (−1)	1204[b] (+1)	1233 (−4)
14,15-^{13}C	1134[b] (0)	1170[b] (−19)	1202[b] (−1)	1234 (−3)
$C_{10}D$	1133 (−1)	1188 (−1)	1319 (+116)	1232 (−5)
$C_{14}D$	1136 (+2)	1188[b] (−1)	1207[b] (+4)	1302 (+65)

[a] Shifts from unmodified 9-*cis*-retinal PSB are given in parentheses. Spectra were obtained in CCl_4 solution. [b] Frequency was determined by Lorentzian deconvolution.

Table VI: Isorhodopsin Vibrational Frequencies[a]

derivative	fingerprint frequency (cm^{-1})			
unmodified	1154	1206	1206	1242
9-^{13}C	1142[b] (−12)	1206 (0)	1188 (−18)	1242 (0)
10,11-^{13}C	1130 (−24)	1202 (−4)	1202 (−4)	1238 (−4)
13-^{13}C	1152 (−2)	1206 (0)	1206 (0)	1238 (−4)
14,15-^{13}C	1154 (0)	1188 (−18)	1204 (−2)	1238 (−4)
15-^{13}C	1154 (0)	1194 (−12)	1205 (−1)	1240 (−2)
$C_{10}D$	1148 (−6)	1222 (+16)	1344 (+138)	1234 (−8)
$C_{14}D$	1160 (+6)	1194 (−12)	1215 (+9)	1294 (+52)

[a] Shifts from unmodified isorhodopsin are given in parentheses. [b] Frequency was determined by Lorentzian deconvolution.

The conformation of the C_{12}–C_{13} single bond in the protein-bound 11-cis PSB chromophore has been discussed by Callender et al. (1976). They correlated the presence of the mode at 998 cm^{-1} with a 12-s-trans conformation. The shift of the 998-cm^{-1} mode to 873 cm^{-1} in $C_{20}D_3$ rhodopsin (Figure 15, see paragraph at end of paper regarding supplementary material) allows us to assign the 998-cm^{-1} band to the $C_{13}CH_3$ rocking vibration. The reduced frequency of this methyl rock in an 11-cis chromophore has been quantitatively correlated with a C_{12}–C_{13} s-trans single bond (Curry et al., 1985).

9-cis-Retinal PSB. The Raman spectra of 9-cis PSB derivatives are presented in Figure 5, and the isotopic shifts are summarized in Table V. C_{10}–C_{11} stretching character is clearly localized at 1134 cm^{-1} as demonstrated by the 20-cm^{-1} shift of this mode in the 10,11-^{13}C derivative. The C_{14}–C_{15} stretch is assigned at 1189 cm^{-1} on the basis of a shift of 19 cm^{-1} in the 14,15-^{13}C derivative. C_8–C_9 stretching character is delocalized and is observed in modes at 1134 and at 1203 cm^{-1}, which shift by 4 and 5 cm^{-1}, respectively, in the 9-^{13}C derivative. Only the 1203-cm^{-1} mode shows the characteristic coupling with the $C_{10}H$ rock. It shifts up to ~1319 cm^{-1} in the $C_{10}D$ derivative. Hence, we assign the "C_8–C_9 stretch" at 1203 cm^{-1}. In the 13-^{13}C derivative the 1237-cm^{-1} mode shifts 4 cm^{-1}, and minor shifts are observed in the other fin-

[3] The modes at 1216 and 1229 cm^{-1} in $C_{14}D$ rhodopsin correspond to the 1208- and 1221-cm^{-1} modes in $C_{14}D$ 11-cis PSB. One is presumably the C_8–C_9 stretch, and the assignment of the other is unknown at this time.

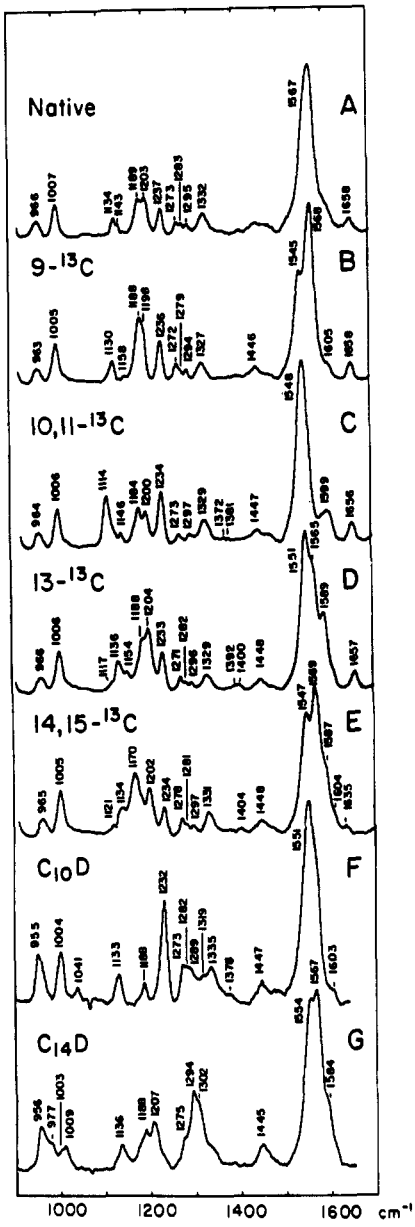

FIGURE 5: Raman spectra of (A) 9-*cis*-retinal protonated Schiff base in CCl_4 solution and its (B) 9-^{13}C, (C) 10,11-^{13}C, (D) 13-^{13}C, (E) 14,15-^{13}C, (F) $C_{10}D$, and (G) $C_{14}D$ derivatives.

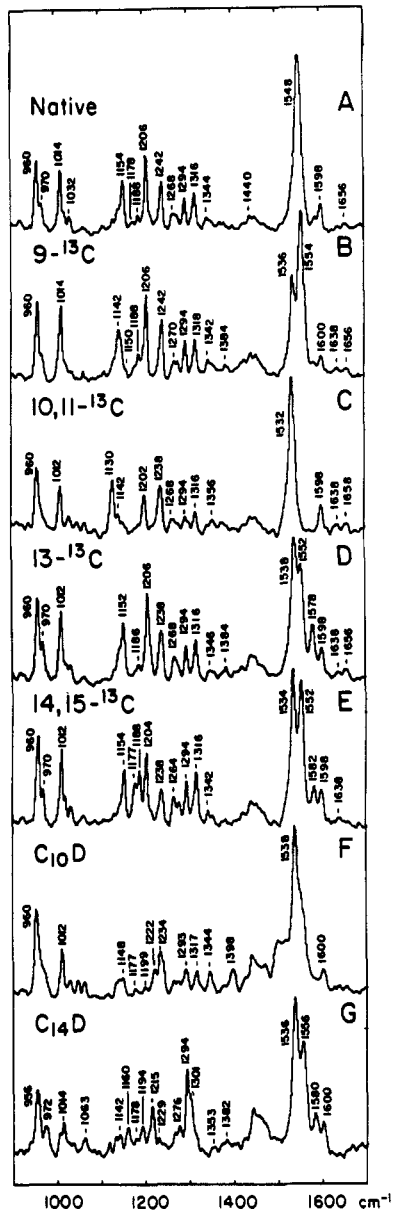

FIGURE 6: Raman spectra of (A) isorhodopsin and its (B) 9-^{13}C, (C) 10,11-^{13}C, (D) 13-^{13}C, (E) 14,15-^{13}C, (F) $C_{10}D$, and (G) $C_{14}D$ derivatives at 77 K (568-nm probe). The $C_{10}D$ spectrum is reproduced from Eyring et al. (1982).

gerprint modes (Table V). Only the 1237-cm^{-1} mode shows coupling with the $C_{14}H$ rock, shifting up to ~1302 cm^{-1} in the $C_{14}D$ derivative. Thus, we assign the "C_{12}–C_{13} stretch" at 1237 cm^{-1}.

Isorhodopsin. RR spectra of isorhodopsin are presented in Figure 6, and the isotopic shifts are summarized in Table VI. The C_{10}–C_{11} stretch is assigned at 1154 cm^{-1} on the basis of the 24-cm^{-1} shift of this band in the 10,11-^{13}C derivative. The large increase in intensity of the modes at 1177 and 1188 cm^{-1} in the 14,15-^{13}C derivative suggests that C_{14}–C_{15} stretch character has moved down from ~1206 cm^{-1} into the modes at 1178 and 1188 cm^{-1}. The assignment of the C_{14}–C_{15} stretch at ~1206 cm^{-1} is strongly supported by the spectrum of 15-^{13}C isorhodopsin (Figure 7) where a *new* line appears at 1194 cm^{-1}, which is clearly the downshifted C_{14}–C_{15} stretch. The residual intensity left at ~1205 cm^{-1} in these derivatives is presumably the C_8–C_9 mode. On the basis of comparison with the 9-cis PSB, we expect the "C_8–C_9 stretch" to be at ~1206 cm^{-1} degenerate with the C_{14}–C_{15} mode. In 9-^{13}C isorhodopsin, intensity shifts from 1154 cm^{-1} down to 1142 cm^{-1}, and an increase in intensity is observed at 1188 cm^{-1}. These changes

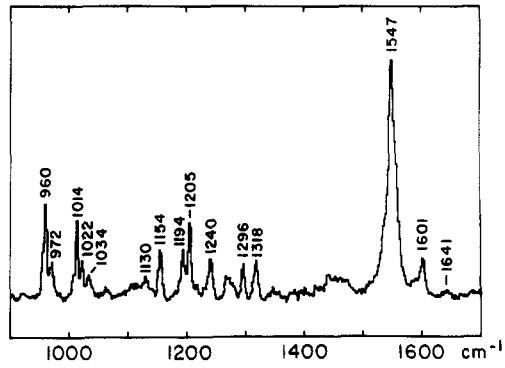

FIGURE 7: Raman spectrum of 15-^{13}C isorhodopsin at 77 K (568-nm probe).

indicate that C_8–C_9 stretch character has moved down into the 1188-cm^{-1} mode and that coupling of the C_8–C_9 with the C_{10}–C_{11} stretch causes a 12-cm^{-1} shift of the 1154-cm^{-1} band. The spectrum of the $C_{10}D$ derivative supports the assignment of the "C_8–C_9 stretch" at 1206 cm^{-1}. A loss of intensity at

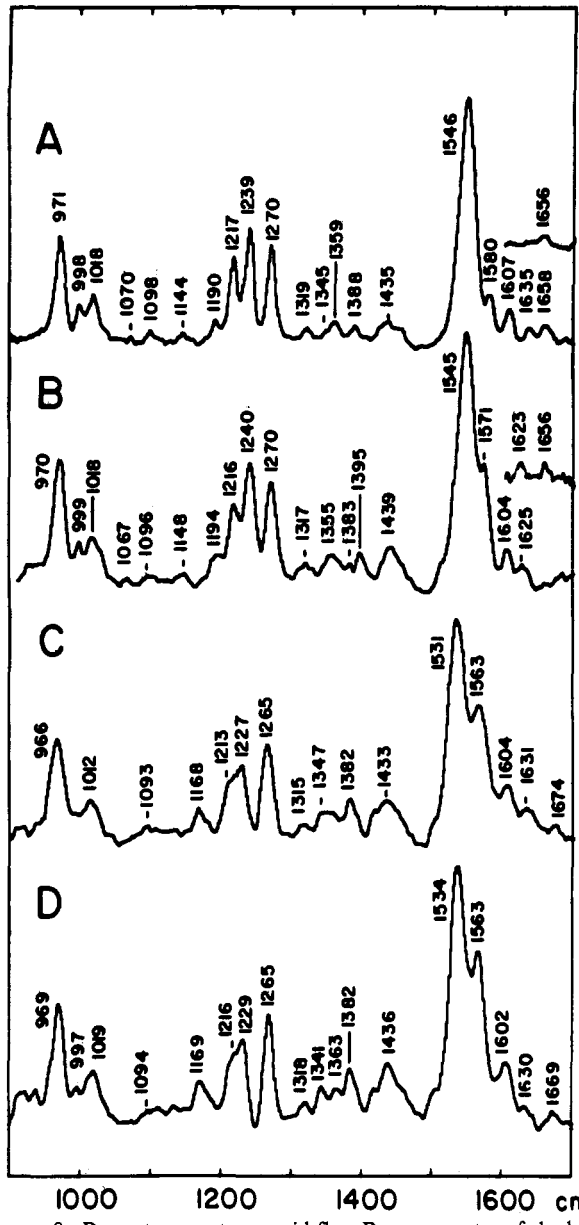

FIGURE 8: Room temperature rapid-flow Raman spectra of rhodopsin in (A) H_2O and (B) D_2O and of 14,15-^{13}C rhodopsin in (C) H_2O and (D) D_2O (488-nm probe). The inserts in (A) and (B) give the Schiff base region probed at 647 nm.

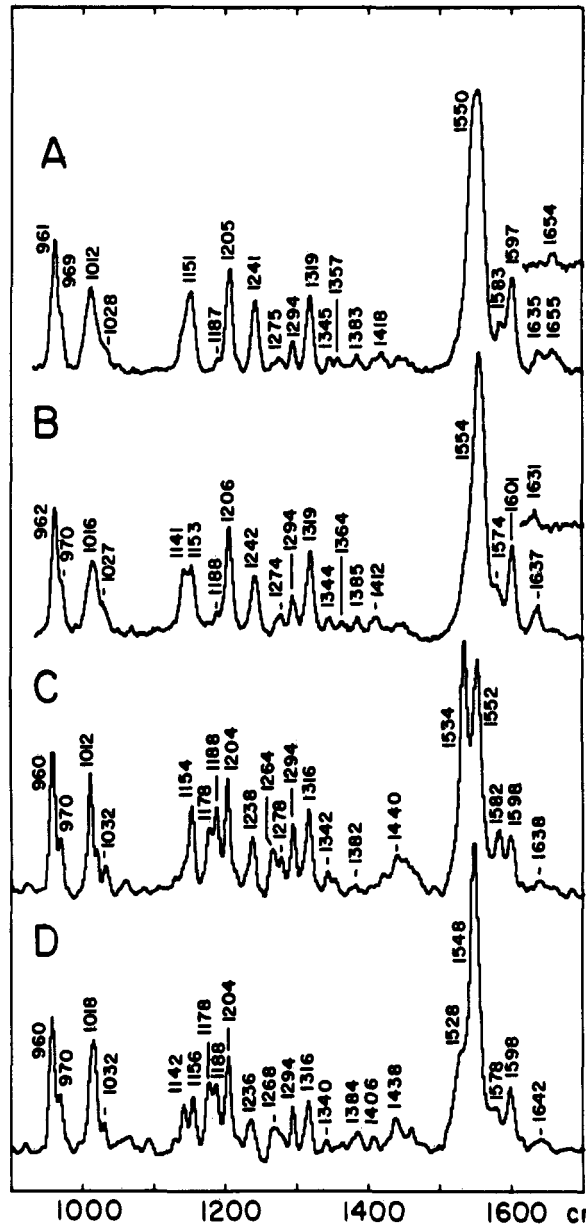

FIGURE 9: Room temperature rapid-flow Raman spectra of isorhodopsin in (A) H_2O and (B) D_2O (488-nm probe). The inserts in (A) and (B) give the Schiff base region probed at 568 nm. Raman spectra of 14,15-^{13}C isorhodopsin at 77 K in (C) H_2O and (D) D_2O (568-nm probe).

1206 cm^{-1} is observed as well as an intensity increase at 1344 cm^{-1} due to the upshifted C_8–C_9 stretching character. In this derivative the C_{14}–C_{15} stretch has presumably shifted up to 1222 cm^{-1}. In 13-^{13}C isorhodopsin a 4-cm^{-1} shift of the 1242-cm^{-1} band is observed. In $C_{14}D$ isorhodopsin, the 1242-cm^{-1} mode shifts up to ~1294 cm^{-1}. Hence, we assign the "C_{12}–C_{13} stretch" at 1242 cm^{-1}. The C_{14}–C_{15} and the C_8–C_9 modes in the $C_{14}D$ pigment are observed at 1194 and 1215 cm^{-1}.

C=N Configuration. The configuration of the C=N double bond can be determined from the sensitivity of the C_{14}–C_{15} stretching coordinate to deuteriation of the Schiff base nitrogen. Normal mode calculations have shown that a trans C=N configuration results in a small shift (~5 cm^{-1}) of the C_{14}–C_{15} stretch upon N-deuteriation, whereas a large (~50-cm^{-1}) shift is observed in a cis C=N configuration. The technique was first applied to intermediates in the photocycle of bacteriorhodopsin (Smith et al., 1984), and the conclusions are in agreement with solid-state NMR results (Harbison et al., 1984).

Figure 8 shows room temperature rapid-flow spectra of rhodopsin and its ND, 14,15-^{13}C, and 14,15-^{13}C,ND derivatives. ND rhodopsin shows only small shifts in the normal modes at 1190 and 1239 cm^{-1}, which contain C_{14}–C_{15} stretching character. Deuteriation of 14,15-^{13}C rhodopsin has no significant effect on the modes at 1168 and 1227 cm^{-1} which contain C_{14}–C_{15} character, either. Since a small shift of the C_{14}–C_{15} stretch correlates with a trans C=N configuration, we conclude that rhodopsin contains a trans (anti) C=N double bond.

Figure 9 gives the corresponding room temperature rapid-flow spectra of isorhodopsin. N-Deuteriation has no effect on the modes at 1205 and at 1241 cm^{-1}, which contain C_{14}–C_{15} stretching character. The frequencies of the fingerprint normal modes at 1178 and 1188 cm^{-1} in 14,15-^{13}C isorhodopsin are also unaffected by N-deuteriation. This demonstrates that isorhodopsin also contains a trans C=N double bond.

Figure 10 presents the spectra of bathorhodopsin. ND bathorhodopsin shows no significant increase in frequency of

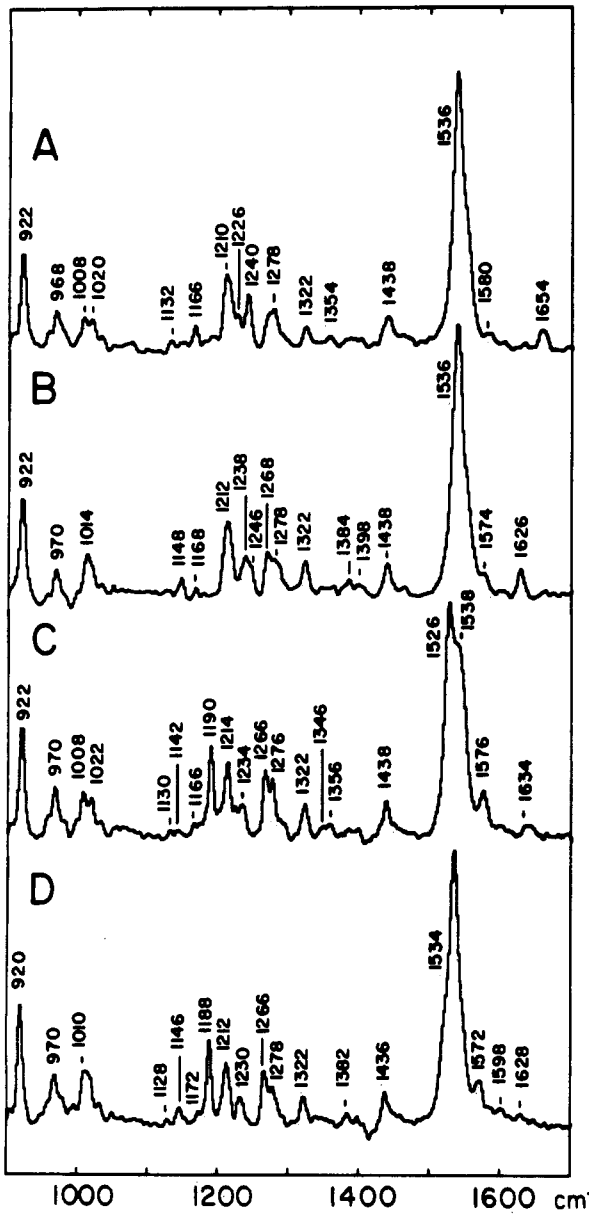

FIGURE 10: Raman spectra of bathorhodopsin in (A) H_2O and (B) D_2O and of 14,15-^{13}C bathorhodopsin in (C) H_2O and (D) D_2O (568-nm probe).

the modes that contain C_{14}–C_{15} stretching character at 1210 and 1240 cm^{-1}. Similarly, the modes at 1190 and 1234 cm^{-1} in 14,15-^{13}C bathorhodopsin show only small shifts upon N-deuteriation. We conclude that bathorhodopsin also contains a trans C=N double bond. Our conclusion that the C=N configurations are trans in all three pigments is in agreement with the FTIR results of Bagley et al. (1985).

C=NH and C=ND Frequencies. The magnitude of the isotopic shift of the C=N stretching mode upon N-deuteriation gives information about the Schiff base environment. In bathorhodopsin we observe a C=NH frequency of 1654 cm^{-1} and a C=ND frequency of 1626 cm^{-1} (Figure 10). Rapid-flow 488-nm probe spectra of rhodopsin and isorhodopsin give C=NH frequencies of 1658 and 1655 cm^{-1}, respectively (Figures 8 and 9). However, with 488-nm excitation, a mode at ~1635 cm^{-1} interferes with the determination of the frequency of the C=ND mode. When longer wavelength laser excitation is used, the interfering 1635-cm^{-1} mode has little Raman intensity. With 647-nm excitation, rhodopsin shows a C=NH stretch at 1656 cm^{-1} and a C=ND stretch at 1623 cm^{-1} (insets to Figure 8). With 568-nm excitation, isorhodopsin has a C=NH stretch at 1654 cm^{-1} and a C=ND stretching frequency at 1631 cm^{-1} (insets to Figure 9). The C=NH and C=ND stretching frequencies measured here are compared with previous measurements in Table VII.

Table VII: Schiff Base Frequencies in H_2O and D_2O

pigment	C=NH (cm^{-1})	C=ND (cm^{-1})	shift (cm^{-1})
rhodopsin	1656[c]	1623[c]	32–35
	1658[b]	1624[f]	
bathorhodopsin	1654[a]	1626[a]	28–33
	1657[e]	1625[e]	
		1624[f]	
isorhodopsin	1654[d]	1631[d]	23–25
	1656[a]	1631[f]	
	1655[b]		
all-trans PSB (methanol)	1658[g]	1632[f]	24

[a] The 77K 568-nm probe experiment. [b] Room temperature 488-nm probe experiment. [c] Room temperature 647-nm probe experiment. [d] Room temperature 568-nm probe experiment. [e] Eyring and Mathies (1979). [f] Bagley et al. (1985). [g] Room temperature 514.5-nm probe experiment.

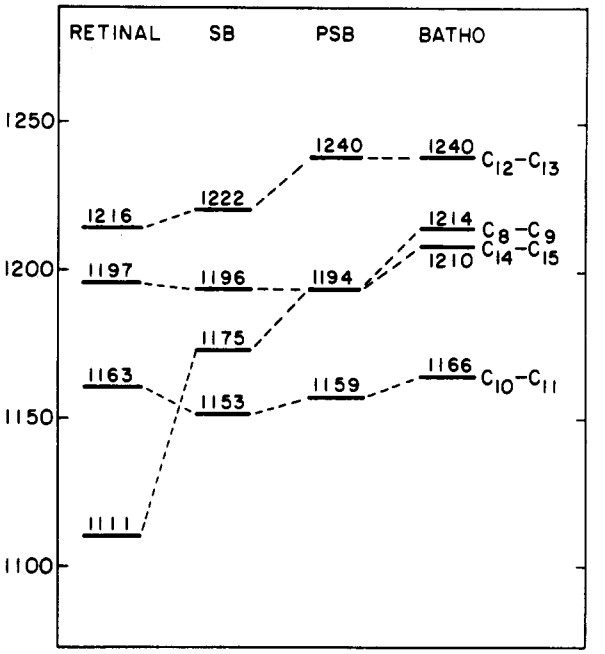

FIGURE 11: Fingerprint correlation diagram for *all-trans*-retinal, its Schiff base (SB), its protonated Schiff base (PSB) in methanol, and bathorhodopsin.

Discussion

Single Bond Conformations in Bathorhodopsin. The "concerted twist" model for the formation of bathorhodopsin proposes that the rhodopsin → bathorhodopsin transition involves an 11-cis,10-s-trans → 11-trans,10-s-cis isomerization (Liu & Asato, 1985). This model can be experimentally tested since the frequency of a C–C stretch is sensitive to conformation. The frequency of a C–C stretching mode in an s-cis structure is expected to be ~100 cm^{-1} below that of its s-trans conformer (Smith et al., 1986). This method has recently been used to argue that the K and L intermediates in the photocycle of bacteriorhodopsin are C_{14}–C_{15} s-trans. Since the C_{10}–C_{11} bond is structurally comparable to the C_{14}–C_{15} bond, similar behavior is expected upon s-cis isomerization.

In Figure 11 the fingerprint normal modes of bathorhodopsin are correlated with those of *all-trans*-retinal, its Schiff base, and its protonated Schiff base. In this correlation diagram and those that follow, the PSB frequencies have been

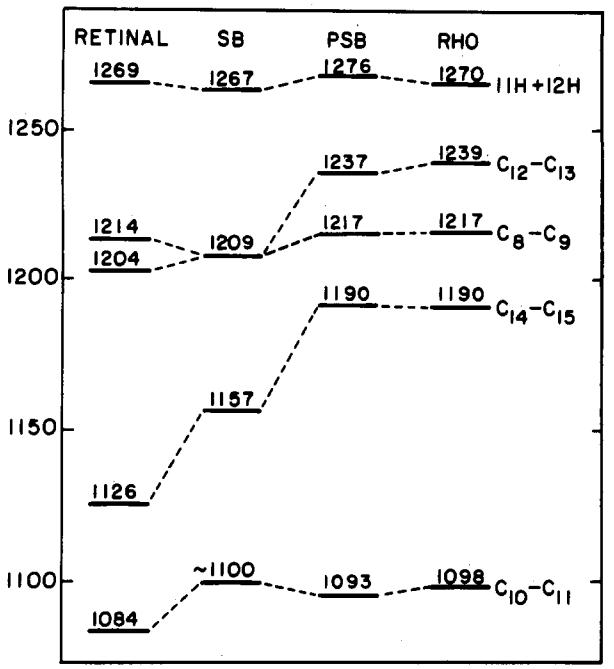

FIGURE 12: Fingerprint correlation diagram for 11-*cis*-retinal, its Schiff base, its protonated Schiff base in methanol, and rhodopsin. The 1270-cm^{-1} band of rhodopsin has been assigned to the $C_{11}H + C_{12}H$ in-plane rock combination (Eyring et al., 1982).

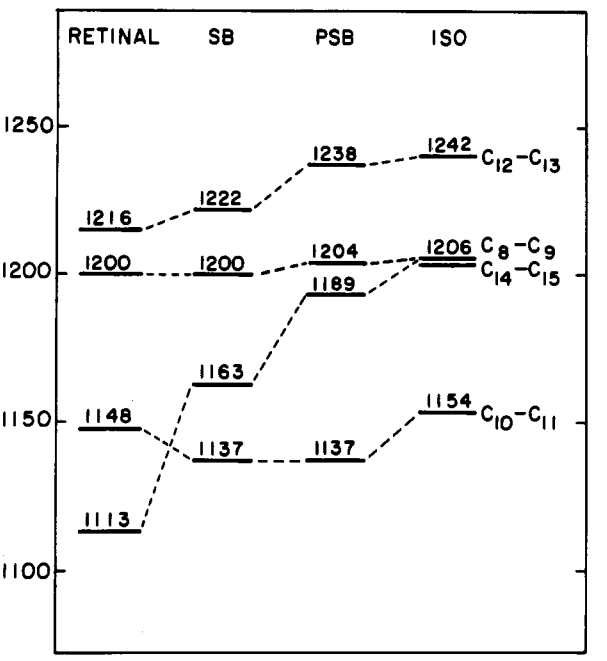

FIGURE 13: Fingerprint correlation diagram for 9-*cis*-retinal, its Schiff base, its protonated Schiff base in methanol, and isorhodopsin.

obtained from spectra recorded in methanol solution since this provides a common reference for protein-induced shifts. The corresponding modes of bathorhodopsin and of the all-trans PSB are all less than 20 cm^{-1} apart, and those of bathorhodopsin are higher in frequency. In particular, the C_{10}–C_{11} stretch of bathorhodopsin (1166 cm^{-1}) is 7 cm^{-1} above its frequency in the all-trans PSB (1159 cm^{-1}). If bathorhodopsin were C_{10}–C_{11} s-cis, the C_{10}–C_{11} stretch would be expected to lie below 1100 cm^{-1}. The "concerted twist" model is therefore incompatible with our data. Furthermore, the fact that the C_{14}–C_{15} stretch in bathorhodopsin is ~16 cm^{-1} above its frequency in the PSB indicates that the C_{14}–C_{15} single bond is also s-trans. *Our data provide compelling evidence against any model in which the C_{10}–C_{11} or C_{14}–C_{15} bond is in the s-cis conformation in bathorhodopsin.*[4] On the basis of less complete assignments of the FTIR spectra of bathorhodopsin, Bagley et al. (1985) have also concluded that the C_{10}–C_{11} conformation in bathorhodopsin is s-trans. Recent locked retinal analogue experiments also do not support the concerted twist model (Asato et al., 1986; Sheves et al., 1986).

It is also interesting to investigate the presence of s-cis bonds in rhodopsin. Figure 12 presents a correlation diagram for 11-cis model compounds and rhodopsin. The extremely close frequency correspondence between the modes of the 11-cis PSB and rhodopsin is striking. Consequently, we conclude that the C_{10}–C_{11} and C_{14}–C_{15} single bonds in rhodopsin are also s-trans. Furthermore, the frequency of the C_{13}–CH_3 rocking vibration (998 cm^{-1}) provides compelling evidence for a C_{12}–C_{13} s-trans conformation, consistent with the conclusion of Callender et al. (1976).

Figure 13 correlates the normal modes of the 9-cis model compounds and isorhodopsin. The fingerprint modes of isorhodopsin are also observed at higher frequency than those of the 9-cis PSB. Therefore, we conclude that the C_{10}–C_{11} and C_{14}–C_{15} single bonds in isorhodopsin are also s-trans.

Opsin Shift Mechanism of Rhodopsin and Isorhodopsin. (*A*) *Fingerprint Region.* Measurements of the opsin shift of dihydroretinal-containing rhodopsin analogues suggested the presence of a negatively charged protein residue near C_{13} (Arnaboldi et al., 1979; Honig et al., 1979a). Such a perturbation is predicted to increase the π-bond order of the C_{14}–C_{15} bond by ~20% (Kakitani et al., 1983). However, no increase of the 1190-cm^{-1} C_{14}–C_{15} stretching mode is observed upon protein binding. In fact, the frequencies (see Figure 12) and dominant C–C stretch character (compare shifts in Tables III and IV) of all the fingerprint modes of the 11-cis PSB are nearly unperturbed by protein binding. Recent solid-state NMR experiments with 14-^{13}C-labeled rhodopsin show that the isotropic chemical shift of C_{14} in rhodopsin is also very similar to the chemical shift of C_{14} in the PSB (Smith et al., 1987a). Therefore, neither the Raman nor the NMR results obtained thus far support the presence of a protein charge perturbation near C_{13} in rhodopsin.

In contrast, comparison of the fingerprint modes of isorhodopsin with those of the 9-cis PSB (Figure 13) shows significant effects on the C_{10}–C_{11} and C_{14}–C_{15} stretching modes, both of which shift up by 17 cm^{-1} upon protein binding. Hence, in isorhodopsin we find evidence for chromophore–protein interaction at several sites along the polyene chain. This suggests that the mechanism of the opsin shift in isorhodopsin may be different from that in rhodopsin.

(*B*) *Schiff Base Region.* Blatz et al. (1972) proposed that a weakened Schiff base–counterion interaction could be responsible for the opsin shift of rhodopsin. This has recently been argued to be the primary mechanism for the opsin shift in BR_{568} (Spudich et al., 1986; Lugtenburg et al., 1986). The reduced ND shift of the C=N mode in BR_{568} (16 cm^{-1}; Smith et al., 1987b) compared to that in the PSB (24 cm^{-1}) seems to be correlated with a weakened hydrogen bond between the

[4] Tavan and Schulten (1986) have recently published an analysis showing that increasing the separation between the Schiff base moiety and its counterion can induce a more delocalized electronic structure that may mask the expected lowering of the C–C stretching frequency in s-cis structures. This effect is probably not significant for the C_{10}–C_{11} mode in bathorhodopsin since the effect is smaller for C–C bonds further from the Schiff base. Their calculations show that increasing the Schiff base–counterion distance from 2 Å to ∞ increases the frequency of the C_{10}–C_{11} mode by only 29 cm^{-1} in the all-trans PSB. This must be considered an upper limit since in the calculation a negative point-charge perturbation was placed near C_5 to enhance the polarization of the electronic structure.

Schiff base and its counterion (Harbison et al., 1983; Hildebrandt & Stockburger, 1984). The C=NH frequencies of the PSB, rhodopsin, and isorhodopsin are within 4 cm^{-1} of each other (Table VII). However, the ND shift of the C=N stretching vibration of rhodopsin (32–35 cm^{-1}) is quite different from the other two (23–25 cm^{-1}).[5] Whatever the explanation for the greatly increased ND shift of rhodopsin, the Schiff base vibrational properties of rhodopsin are significantly different from those of the PSB. This suggests that an altered Schiff base environment may be involved in the opsin shift mechanism of rhodopsin. Also, the fact that the ND shifts of rhodopsin and isorhodopsin are different suggests again that the mechanism of the opsin shift might be different in these two pigments.

Energy Storage in Bathorhodopsin. The configuration and electrostatic environment of the protonated Schiff base linkage and the location and nature of specific chromophore–protein interactions are also of importance in understanding the mechanism of energy storage in bathorhodopsin. It has been proposed that this energy is stored by electrostatic interactions between the protonated Schiff base and the local protein environment (Honig et al., 1979b; Warshel & Barboy, 1982; Birge & Hubbard, 1980). These models require the electrostatic environment of the Schiff base moiety in bathorhodopsin to be different from that in rhodopsin. Since we have determined that the primary photochemistry does *not* involve C=N isomerization, 11-cis → 11-trans isomerization implies that a reorientation of the Schiff base proton takes place during the primary photochemistry. However, one would expect the C=NH and C=ND stretching frequencies to be sensitive to such a difference in environment. This sensitivity has been observed in the primary photochemistry of bacteriorhodopsin, where the C=NH stretching frequency changes by ~20 cm^{-1} in the BR_{568} → K transition and large changes in the ND-induced shift are observed (Rothschild et al., 1984; Stern & Mathies, 1986; Terner et al., 1979). We fail to observe such large changes in C=N vibrational properties during the primary photochemistry of rhodopsin. The C=NH stretching frequencies of rhodopsin and bathorhodopsin are identical within experimental error, and the ND shifts differ by only ~5 cm^{-1}. The decreased ND shift of bathorhodopsin suggests that the Schiff base hydrogen bond is somewhat weaker in bathorhodopsin than in rhodopsin. Although a small perturbation is observed, our C=N data do not support the idea that a major fraction of the 36 kcal/mol of energy stored in bathorhodopsin is stored in the form of electrostatic energy between the protonated Schiff base and the local protein environment.

This apparent paradox may be resolved in part by the space-filling models in Figure 14 depicting the rhodopsin → bathorhodopsin transition. Here we have constrained the ionone ring and the α-carbon of lysine to lie as close as possible in the same position after having performed the formal C_{11}=C_{12} cis → trans isomerization. We have incorporated a 20° twist about the C_{12}–C_{13} bond in rhodopsin. This is the expected minimum energy conformation for an 11-cis,12-s-trans structure. Bathorhodopsin is shown with 20° twists around the C_{10}–C_{11}, C_{12}–C_{13}, and C_{14}–C_{15} bonds, which are necessary to explain the Raman intensity of the HOOP wags

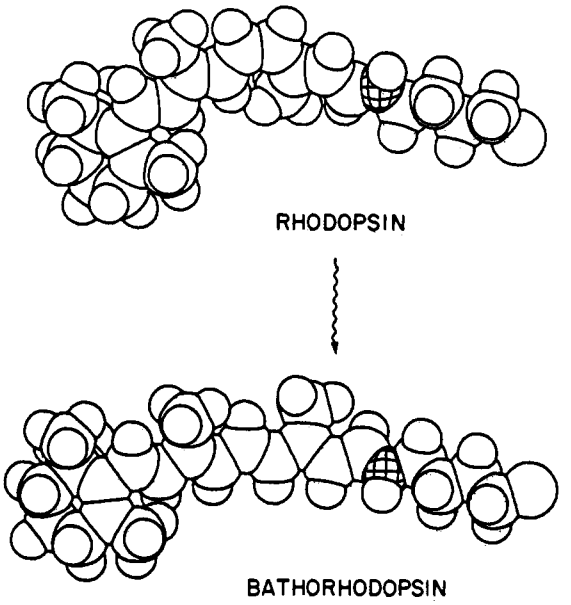

FIGURE 14: Rhodopsin and bathorhodopsin model structures. Rhodopsin is shown in a twisted C_{12}–C_{13} s-trans form. The C_{11}=C_{12} trans bathorhodopsin structure is distorted by applying 20° twists in the same direction about the C_{10}–C_{11}, C_{12}–C_{13}, and C_{14}–C_{15} bonds.

(Eyring et al., 1982). This gives an ~45° dihedral angle between the two methyl groups in bathorhodopsin. As a result of these conformational twists, the spatial difference between the two chromophores is much less than one would naively expect for a formal cis → trans isomerization, and the Schiff base proton remains in nearly the same environment after isomerization. This provides a rationalization for how the Schiff base properties can remain so constant while "N–H reorientation" occurs.

In the fingerprint and HOOP regions of the RR spectrum of bathorhodopsin we do find evidence for chromophore–protein interactions that may be involved in the energy storage mechanism. First, the C_8–C_9 and C_{14}–C_{15} stretching frequencies shift up by 20 and 16 cm^{-1} compared with those in the PSB (Figure 11). Protein perturbations affecting the frequencies of the C_8–C_9 and C_{14}–C_{15} modes of bathorhodopsin can be electrostatic in nature (increasing the bond order; Kakitani et al., 1983) or can result from chromophore perturbations such as CCC valence angle distortions (I. Palings and R. A. Mathies, unpublished results). Second, in the low-wavenumber region of the spectrum we find intense hydrogen out-of-plane wagging vibrations, which have been assigned to the C_{10}H, C_{11}H, C_{12}H, and C_{14}H wags (Eyring et al., 1982). Intensity in these modes results from out-of-plane distortions of the chromophore such as CCCC torsions (Warshel & Barboy, 1982; Eyring et al., 1980). Finally, in bathorhodopsin the C_{11}H and C_{12}H wags are anomalously uncoupled due to the fact that the C_{12}H wag is much lower in frequency than the C_{11}H wag (Eyring et al., 1982). Out-of-plane distortion of the C_{11}=C_{12} double bond appears to be insufficient to uncouple the C_{11}H and C_{12}H out-of-plane wags (Warshel & Barboy, 1982). Theoretical studies on the effects of proximate charges and chromophore distortions on the vibrational spectrum are needed to model these observations. A successful model must account for both the energy storage and the unusual vibrational properties of the bathorhodopsin chromophores.

Summary and Conclusions

Comparison of the fingerprint modes of visual pigments and their model compounds shows that the C_{10}–C_{11} and C_{14}–C_{15}

[5] The increased ND shift of rhodopsin (32–35 cm^{-1}) suggests a strengthening of the Schiff base hydrogen bond relative to the PSB in methanol. Increased hydrogen bonding is expected to counteract the red shift of rhodopsin. However, a quantitative relationship between the ND shift of the C=N stretch and its hydrogen-bonding environment has not yet been established. [For a discussion of the vibrational properties of the Schiff base, see López-Garriga et al. (1986) and Aton et al. (1980).]

single bonds are s-trans in rhodopsin, bathorhodopsin, and isorhodopsin. This provides compelling evidence against the model of bathorhodopsin proposed by Liu and Asato (1985), which suggests a C_{10}–C_{11} s-cis structure. Furthermore, the insensitivity of the C_{14}–C_{15} stretching mode to N-deuteriation in all three pigments demonstrates that each contains a trans (anti) protonated Schiff base bond.

The extreme similarity of the fingerprint frequencies of rhodopsin and the 11-cis PSB does not support the presence of a negatively charged protein residue near C_{13}, which is thought to be responsible for the opsin shift. However, the unusually large ND shift of the Schiff base mode in rhodopsin relative to the PSB in methanol suggests that the opsin shift mechanism may involve the Schiff base. In contrast, large perturbations of the C_{10}–C_{11} and C_{14}–C_{15} fingerprint modes are observed in isorhodopsin, while the C=NH and C=ND stretching frequencies are essentially identical with those of the PSB. This suggests that the mechanism for the opsin shift may be different in rhodopsin and isorhodopsin.

The modest difference between the Schiff base vibrational properties of rhodopsin and bathorhodopsin is inconsistent with the idea that energy storage in bathorhodopsin is associated with an altered Schiff base environment. The increased C_8–C_9 and C_{14}–C_{15} stretching frequencies and the anomalous properties of the hydrogen out-of-plane wagging vibrations indicate that chromophore–protein interactions in the center of the chain are involved in the energy storage mechanism.

Acknowledgments

We thank W. Thomas Pollard for assistance in preparing the space-filling drawings, Steven O. Smith for providing the all-trans PSB data, and Bo Curry for stimulating discussions.

Supplementary Material Available

Figure 15 presenting the room temperature rapid-flow spectrum (488-nm probe) of $C_{20}D_3$ rhodopsin from 800 to 1600 cm^{-1} (1 page). Ordering information is given on any current masthead page.

References

Applebury, M. L., Zuckerman, D. M., Lamola, A. A., & Jovin, T. M. (1974) *Biochemistry 13*, 3448.

Arnaboldi, M., Motto, M. G., Tsujimoto, K., Balogh-Nair, V., & Nakanishi, K. (1979) *J. Am. Chem. Soc. 101*, 7082.

Asato, A. E., Denny, M., & Liu, R. S. H. (1986) *J. Am. Chem. Soc. 108*, 5032.

Aton, B., Doukas, A. G., Narva, D., Callender, R. H., Dinur, U., & Honig, B. (1980) *Biophys. J. 29*, 79.

Bagley, K. A., Balogh-Nair, V., Croteau, A. A., Dollinger, G., Ebrey, T. G., Eisenstein, L., Hong, M. K., Nakanishi, K., & Vittitow, J. (1985) *Biochemistry 24*, 6055.

Bennett, N., Michel-Villaz, M., & Kuhn, H. (1982) *Eur. J. Biochem. 127*, 97.

Birge, R. R., & Hubbard, L. M. (1980) *J. Am. Chem. Soc. 102*, 2195.

Birge, R. R., & Hubbard, L. M. (1981) *Biophys. J. 34*, 517.

Blatz, P. E., Mohler, J. H., & Navangul, H. V. (1972) *Biochemistry 11*, 848.

Boucher, F., & LeBlanc, R. M. (1985) *Photochem. Photobiol. 41*, 459.

Braiman, M., & Mathies, R. (1982) *Proc. Natl. Acad. Sci. U.S.A. 79*, 403.

Callender, R. H., Doukas, A., Crouch, R., & Nakanishi, K. (1976) *Biochemistry 15*, 1621.

Chabre, M. (1985) *Annu. Rev. Biophys. Biophys. Chem. 14*, 331.

Cooper, A. (1979) *Nature (London) 282*, 531.

Curry, B., Broek, A., Lugtenburg, J., & Mathies, R. (1982) *J. Am. Chem. Soc. 104*, 5274.

Curry, B., Palings, I., Broek, A. D., Pardoen, J. A., Lugtenburg, J., & Mathies, R. (1985) *Adv. Infrared Raman Spectrosc. 12*, 115.

Eyring, G., & Mathies, R. (1979) *Proc. Natl. Acad. Sci. U.S.A. 76*, 33.

Eyring, G., Curry, B., Mathies, R., Fransen, R., Palings, I., & Lugtenburg, J. (1980) *Biochemistry 19*, 2410.

Eyring, G., Curry, B., Broek, A., Lugtenburg, J., & Mathies, R. (1982) *Biochemistry 21*, 384.

Freedman, K. A., & Becker, R. S. (1986) *J. Am. Chem. Soc. 108*, 1245.

Harbison, G. S., Herzfeld, J., & Griffin, R. G. (1983) *Biochemistry 22*, 1.

Harbison, G. S., Smith, S. O., Pardoen, J. A., Winkel, C., Lugtenburg, J., Herzfeld, J., Mathies, R., & Griffin, R. G. (1984) *Proc. Natl. Acad. Sci. U.S.A. 81*, 1706.

Hargrave, P. A., McDowell, J. H., Curtis, D. R., Wang, J. K., Juszczak, E., Fong, S.-L., Mohana Rao, J. K., & Argos, P. (1983) *Biophys. Struct. Mech. 9*, 235.

Haynes, L. W., Kay, A. R., & Yau, K.-W. (1986) *Nature (London) 321*, 66.

Hildebrandt, P., & Stockburger, M. (1984) *Biochemistry 23*, 5539.

Honig, B., Dinur, U., Nakanishi, K., Balogh-Nair, V., Gawinowicz, M. A., Arnaboldi, M., & Motto, M. G. (1979a) *J. Am. Chem. Soc. 101*, 7084.

Honig, B., Ebrey, T., Callender, R. H., Dinur, U., & Ottolenghi, M. (1979b) *Proc. Natl. Acad. Sci. U.S.A. 76*, 2503.

Kakitani, H., Kakitani, T., Rodman, H., Honig, B., & Callender, R. (1983) *J. Phys. Chem. 87*, 3620.

Liu, R. S. H., & Asato, A. E. (1985) *Proc. Natl. Acad. Sci. U.S.A. 82*, 259.

Lõpez-Garriga, J. J., Babcock, G. T., & Harrison, J. F. (1986) *J. Am. Chem. Soc. 108*, 7241.

Lugtenburg, J. (1985) *Pure Appl. Chem. 57*, 753.

Lugtenburg, J., Muradin-Szweykowska, M., Heeremans, C., Pardoen, J. A., Harbison, G., Herzfeld, J., Griffin, R. G., Smith, S. O., & Mathies, R. A. (1986) *J. Am. Chem. Soc. 108*, 3104.

Mathies, R., Oseroff, A. R., & Stryer, L. (1976) *Proc. Natl. Acad. Sci. U.S.A. 73*, 1.

Oseroff, A. R., & Callender, R. H. (1974) *Biochemistry 13*, 4243.

Ovchinnikov, Y. A. (1982) *FEBS Lett. 148*, 179.

Palings, I., Mathies, R. A., Pardoen, J. A., Winkel, C., & Lugtenburg, J. (1985) *Biophys. J. 47*, 358a.

Pardoen, J. A., van den Berg, E. M. M., Winkel, C., & Lugtenburg, J. (1986) *Recl.: J. R. Neth. Chem. Soc. 105*, 92.

Rothschild, K. J., Roepe, P., Lugtenburg, J., & Pardoen, J. A. (1984) *Biochemistry 23*, 6103.

Sheves, M., Albeck, A., Ottolenghi, M., Bovee-Geurts, P. H. M., DeGrip, W. J., Einterz, C. M., Lewis, J. W., Schaechter, L. E., & Kliger, D. S. (1986) *J. Am. Chem. Soc. 108*, 6440.

Smith, S. O. (1985) Ph.D. Dissertation, University of California, Berkeley, CA.

Smith, S. O., Myers, A. B., Pardoen, J. A., Winkel, C., Mulder, P. P. J., Lugtenburg, J., & Mathies, R. (1984) *Proc. Natl. Acad. Sci. U.S.A. 81*, 2055.

Smith, S. O., Myers, A. B., Mathies, R. A., Pardoen, J. A., Winkel, C., van den Berg, E. M. M., & Lugtenburg, J. (1985) *Biophys. J. 47*, 653.

Smith, S. O., Hornung, I., van der Steen, R., Pardoen, J. A., Braiman, M., Lugtenburg, J., & Mathies, R. A. (1986) *Proc. Natl. Acad. Sci. U.S.A. 83*, 967.
Smith, S. O., Palings, I., Copié, V., Raleigh, D. P., Courtin, J., Pardoen, J. A., Lugtenburg, J., Mathies, R. A., & Griffin, R. G. (1987a) *Biochemistry 26*, 1606.
Smith, S. O., Braiman, M. S., Myers, A. B., Pardoen, J. A., Courtin, J. M. L., Winkel, C., Lugtenburg, J., & Mathies, R. A. (1987b) *J. Am. Chem. Soc.* (in press).
Smith, S. O., Pardoen, J. A., Lugtenburg, J., & Mathies, R. A. (1987c) *J. Phys. Chem. 91*, 804.
Spudich, J. L., McCain, D. A., Nakanishi, K., Okabe, M., Shimizu, N., Rodman, H., Honig, B., & Bogomolni, R. A. (1986) *Biophys. J. 49*, 479.
Stern, D., & Mathies, R. (1985) *Proceedings in Physics* (Stockburger, M., & Laubereau, A., Eds.) Vol. 4, p 250, Springer-Verlag, New York.
Stryer, L. (1986) *Annu. Rev. Neurosci. 9*, 87.
Suzuki, T., & Callender, R. H. (1981) *Biophys. J. 34*, 261.
Tavan, P., & Schulten, K. (1986) *Biophys. J. 50*, 81.
Terner, J., Hsieh, C.-L., Burns, A. R., & El-Sayed, M. A. (1979) *Proc. Natl. Acad. Sci. U.S.A. 76*, 3046.
Warshel, A., & Barboy, N. (1982) *J. Am. Chem. Soc. 104*, 1469.
Yoshizawa, T., & Wald, G. (1963) *Nature (London) 197*, 1279.
Zimmerman, A. L., & Baylor, D. A. (1986) *Nature (London) 321*, 70.

Energy Storage in the Primary Photochemical Events of Rhodopsin and Isorhodopsin

G. Alan Schick, Thomas M. Cooper, Richard A. Holloway, Lionel P. Murray, and Robert R. Birge*

Department of Chemistry, Carnegie-Mellon University, Pittsburgh, Pennsylvania 15213
Received October 15, 1986; Revised Manuscript Received December 19, 1986

ABSTRACT: The energetics associated with the photoequilibrium

$$\text{rhodospin (R)} \underset{h\nu}{\overset{h\nu}{\rightleftharpoons}} \text{bathorhodopsin (B)} \underset{h\nu}{\overset{h\nu}{\rightleftharpoons}} \text{isorhodopsin (I)}$$

are measured at 77 K by using pulsed-laser photocalorimetry and a range of excitation wavelengths and relative starting concentrations. Enthalpies for the photochemical transformations R $\xrightarrow{h\nu}$ B and I $\xrightarrow{h\nu}$ B are measured to be $\Delta H_{RB} = 32.2 \pm 0.9$ kcal mol^{-1} and $\Delta H_{IB} = 27.1 \pm 3.2$ kcal mol^{-1}, respectively. Although the value of ΔH_{RB} is slightly lower than that reported previously by Cooper of 34.7 ± 2.2 kcal mol^{-1} [Cooper, A. (1979) *Nature (London) 282*, 531–533], the two values are in agreement within experimental error. The energy difference $\Delta H_{RB} - \Delta H_{IB} = 5.1 \pm 3.3$ kcal mol^{-1} is identical within experimental error with the difference in enthalpies of isorhodopsin and rhodopsin [5.2 ± 2.3; Cooper, A. (1979) *FEBS Lett. 100*, 382–384]. We suggest that this result is consistent with the theory that bathorhodopsin is a single, common photochemical intermediate connecting rhodopsin and isorhodopsin.

The primary event in the vertebrate vision process involves absorption of light by the membrane glycoprotein rhodopsin (R) and its conversion to a metastable intermediate, bathorhodopsin (B). The chromophore of R is the protonated Schiff base of 11-*cis*-retinal, which isomerizes to the all-trans form during the primary event (Honig, 1978; Ottolenghi, 1980; Birge, 1981). The photoreaction is endothermic, and the energy stored by B is used to promote subsequent thermal reactions in the protein bleaching sequence and in the subsequent transducin cycle. At physiological temperatures, the protein decays from B through several intermediates and eventually ($\sim 10^3$ s later) dissociates into *all-trans*-retinal and opsin. Complex dark reactions within the transducin cycle then serve to regenerate rhodopsin, and the cycle continues toward the eventual hydrolysis of cyclic GMP to 5′-GMP. This hydrolysis results in a constriction of the flow of Na^+ ions through the rod outer segment, thus hyperpolarizing the retinal rod cell. Vision is produced when this electrical signal is communicated to the other end of the retinal rod cell and to the other cells of the retina (Stryer, 1986).

Bathorhodopsin is stable at 77 K and forms the central species of a three-component photoequilibrium (Yoshizawa & Wald, 1963):

$$\text{R} \underset{h\nu}{\overset{h\nu}{\rightleftharpoons}} \text{B} \underset{h\nu}{\overset{h\nu}{\rightleftharpoons}} \text{I} \qquad \text{(1a)}$$

where isorhodopsin (I) is the label given to the 9-*cis*-retinyl isomer of the protein. The energetics of this photoequilibrium are very important in understanding light transduction in the visual process. The origin of the energy storage remains a subject of active study. Various mechanisms have been proposed whereby energy is stored in the form of either charge separation (Rosenfeld et al., 1977; Honig et al., 1979) or a mixture of charge separation and protein strain (Birge & Hubbard, 1980; Warshel & Barboy, 1982) as a result of the 11-cis to 11-trans photoisomerization of the retinyl chromophore. The energetics of the 11-cis (R) → 11-trans (B) photoconversion have been measured (Cooper, 1979a; Boucher & Leblanc, 1985), but these values are more than double the comparable energy storage associated with the primary event

0006-2960/87/0426-2556$01.50/0